

Battery Pack Modeling and Performance Assessment for Electric Vehicle Applications

Master's thesis in Automotive Engineering

VINAY SRINIVASAN

DEPARTMENT OF MECHANICS AND MARITIME SCIENCES

CHALMERS UNIVERSITY OF TECHNOLOGY
Gothenburg, Sweden 2021
www.chalmers.se

MASTER'S THESIS 2021

**Battery Pack Modeling and Performance
Assessment for Electric Vehicle Applications**

VINAY SRINIVASAN



CHALMERS
UNIVERSITY OF TECHNOLOGY

DEPARTMENT OF MECHANICS AND MARITIME SCIENCES

Division of Vehicle Engineering and Autonomous Systems

CHALMERS UNIVERSITY OF TECHNOLOGY

Gothenburg, Sweden 2021

Battery Pack Modeling and Performance Assessment for Electric Vehicle Applications

© VINAY SRINIVASAN, 2021.

Supervisor: Majid Astaneh, PhD, Post-Doc Researcher, Division of VEAS, M2, Chalmers

Examiner: Jelena Andric, PhD, Docent, Division of VEAS, M2, Chalmers,

Master's Thesis 2021: 53

Department of Mechanics and Maritime Sciences

Division of Vehicle Engineering and Autonomous Systems

Chalmers University of Technology

SE-412 96 Gothenburg

Telephone +46 31 772 1000

Typeset in L^AT_EX

Printed by Chalmers Reproservice

Gothenburg, Sweden 2021

Battery Pack Modeling and Performance Assessment for Electric Vehicle Applications

VINAY SRINIVASAN

Department of Mechanics and Maritime Sciences
Chalmers University of Technology

Abstract

Large traction battery packs are made up of several number of cells connected in series and parallel to fulfill vehicle demanded voltage and capacity. For many years, the operation of the battery packs has been overestimated by only scaling up battery cell performance to mimic pack behavior. The inconsistencies in the current, State of Charge (SOC) and temperature of the individual cells/modules originating from the battery pack electrical topology and thermal circuit design, negatively influence the pack overall performance. In the current thesis work, lumped battery pack is modified to account for cell-to-cell variations. All simulations have been performed in Siemens Amesim, a commercial software for the modeling and analysis of multi-domain systems.

The inhomogeneities within the battery pack are modeled by considering interconnection resistance between parallel branches. The input current to the models is given either as a constant value or through a current profile obtained from literature survey and the software tutorial. Both the lumped pack and cell-to-cell discretized models (C2C) are compared in terms of model predictability. The results show that with C2C model the variations between the cells can be observed and quantified. The C2C model discharges 11% faster compared to the lumped pack model when Worldwide harmonized Light-duty vehicles Test Procedure(WLTP) current profile is inputted. The maximum temperature attained by C2C model is 12 °C greater than the lumped pack model. It can be concluded that when lumped pack modelling approach is employed the vehicle achievable range is overestimated and the maximum temperature is underestimated.

Keywords: Battery pack modelling, Equivalent circuit method, cell-to-cell variations, electric vehicle.

Acknowledgements

I am grateful to my examiner Jelena Andric and my supervisor Majid Astaneh for providing me an opportunity to do thesis under their guidance. I would like to thank my supervisor Majid Astaneh for giving me great knowledge, suggestions and feedback. I am so grateful for his patience. I am also grateful for my examiner Jelena Andric for giving suggestions, references and feedbacks.

I would like to thank Gunnar Latz and Christopher Helbig for providing me suggestions for developing the battery model. Finally, I wish to recognize and so much grateful for my family and friends for their constant support, which has kept me motivated and helped me in this work.

Vinay Srinivasan, Gothenburg, June,2021

Abbreviation

BEV	Battery Electric vehicle
SOC	State of Charge
SOH	State of health
OCV	Open circuit voltage
ECM	Equivalent circuit modelling
C2C	Cell to cell discretized model
WLTP	Worldwide harmonized Light-duty vehicles Test Procedure

List of symbols

A	Cell surface area (m^2)
c_p	specific heat ($J kg^{-1} K^{-1}$)
h	heat transfer coefficient ($W/m^2/ ^\circ C$)
I	Current (A)
R_{IC}	Interconnection resistance (Ohm)
R_{int}	Internal resistance (Ohm)
t	Time (s)
T	Temperature ($^\circ C$)
V	Voltage (V)



Contents

1	Introduction	1
1.1	Background	1
1.2	Problem Statement	2
1.3	Previous work	2
1.4	Goal Statement	2
2	Theory and background information	3
2.1	Lithium-ion battery	3
2.1.1	Battery Cells	3
2.1.2	Battery packs	4
2.2	Terminologies	5
3	Methodology	7
3.1	Cell electrical-thermal modelling	7
3.1.1	Equivalent circuit method (ECM)	7
3.1.2	Thermal modelling	8
3.1.2.1	Heat generation	8
3.2	Lumped pack approach	9
3.3	Cell-to-cell descritization approach	9
3.4	Cell Specification	11
3.5	Case setup	11
3.5.1	Case 1- Constant discharge current	11
3.5.2	Case2- Current profile from test rig	11
3.5.3	Case 3-WLTP class 3	12
4	Results and discussion	13
4.1	Case 1- Constant current source	13
4.1.1	1 C discharge	13
4.1.2	5 C discharge	15
4.2	Case 2- Current profile from test rig	17
4.3	Case 3 - WLTP class 3	19
4.3.1	Normal condition	19
4.3.2	Faulty condition	22
5	Conclusion and future work	25

1

Introduction

1.1 Background

Recently, the automotive sector has faced a paradigm shift towards electromobility to fulfill the requirements of the sustainable modern society [1]. Carbon dioxide emission has reached 50 billion tonnes per year which has increased by 40% compared to 1990 [2]. Figure 1.1 shows that 74% of transport emissions come from road vehicles [3]. So the OEM's are heading towards developing a sustainable transportation mode and battery electric vehicles (BEVs) are taking the lead.

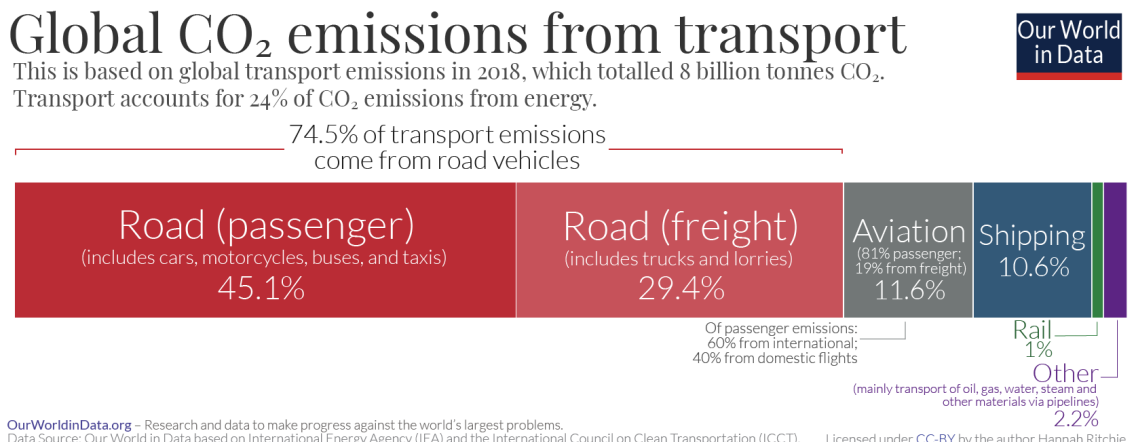


Figure 1.1: Carbon dioxide emissions from transportation vehicles [2]

Lithium-ion batteries have gained more popularity in recent years due to their high energy density, low self-discharge rate and prolonged life compared to other types of batteries [25]. The predominant challenges for BEV are to provide long-range, development of fast charging infrastructures and efficient operation of the system under different environmental conditions. To address these limitations, many OEMs have developed various simulation tools where the electric vehicle can be modelled systematically and its performance can be assessed under different working scenarios. At the subsystem level the battery pack performance can be predicted and optimised using the aforesaid simulation tools [26].

1.2 Problem Statement

To achieve certain voltage and capacity, battery packs are made up of several hundreds of cells connected in series and parallel. In modelling of battery packs, lumped approach model has been employed for many years where the cell model is scaled up to resemble battery pack. With this approach it is not possible to understand cell-to-cell variations, which play a key role in the energy and thermal performance of battery packs. Developing a cell-to-cell discretised battery pack model (C2C model) provides detailed insight about battery pack performance under real life working scenarios and hence brings forth guidelines in designing energy and thermally efficient battery packs.

1.3 Previous work

There are different approaches in modelling and simulation of battery cells depending on the application under consideration [9]. The main types of battery cell modelling are electrochemical modelling, equivalent electric circuit modelling and neural Network modelling [15]. Among them, equivalent circuit models are most commonly used because of reduced complexity and ability to provide good results [12]. A battery pack has several cells in series and parallel. To increase the capacity of the battery pack, cells are connected in parallel [16]. Cells in the battery pack don't behave equally, the variations between them cause differences in state of charge (SOC), state of health (SOH) and capacity which ultimately affect the long term performance and leads to localized ageing in the pack which in turn amplifies the inhomogeneities in large traction battery packs [17] [18]. For cells connected in series, it is possible to control each one of them by passive or active balancing modules [19] [20], whereas it is difficult for cells connected in parallel [21]. Bruen et al.[16], in their research work conclude that when cells are connected in parallel, the fluctuations in current occurs which will affect the ageing of the cell. Xianzhi Gong et al.[23], mentioned that when cells are connected in parallel with the difference in degradation, there will be capacity loss which further leads to accelerated degradation. Hosseinzadeh et al.[24], developed a battery model with cells connected in parallel with interconnection between them. The authors concluded that the thermal gradient and the change in depth of discharge of the cells increase at higher load currents and with change in interconnection resistance. None of the above-referenced studies evaluated the non-uniformities in battery pack operation under transient current profiles obtained from vehicle applications.

1.4 Goal Statement

The goal of this thesis project is to enhance battery pack model predictability by employing the cell-to-cell discretization approach to evaluate the energy efficiency of the pack under different working scenarios.

2

Theory and background information

This chapter gives knowledge about theoretical concepts used in this thesis.

2.1 Lithium-ion battery

2.1.1 Battery Cells

Lithium-ion batteries are the most commonly used energy source in vehicle applications. An electrochemical cell is the basic component of the battery. It converts chemical energy into electrical energy when discharged and electrical energy into chemical energy when charged. Electrochemical cells are also classified as primary and secondary cells where primary cells can only be discharged and secondary cells can be discharged and charged. The cell geometry and capacity depends on the type of application, but generally, the cell geometry is classified into *Cylindrical*, *Prismatic* and *Pouch* cells [33]. Figure 2.1 shows the different types of commercially available cell geometries.

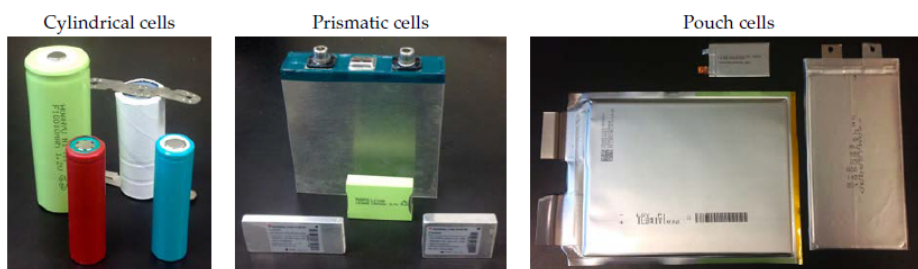


Figure 2.1: Different cell geometries [8]

Figure 2.2 shows a schematic representation of an electrochemical cell sandwich. It consists of a positive electrode, a negative electrode, the separator which separates the positive and negative electrode, the electrolyte that fills the void space within the cell and current collectors. Redox reactions such as oxidation and reduction reactions take place at the interface between the electrodes and electrolyte and are responsible for the charge and discharge process in the cell [8]. Under discharge, at the negative electrode (the anode) the oxidation process takes place where electrons are transferred from the negative electrode towards the positive electrode (the

cathode) through an external circuit and at the cathode the reduction process takes place by accepting the electrons. Usually, graphite is used as anode material and for the cathode, a combination of Li^+ ions with either layered or spinel compounds containing Manganese, Cobalt and Nickel are used [29]. The ions are conducted through **electrolyte**. An electrolyte consists of one or many salts in one or combined solvents. The electrolyte should have high ion conductivity[6].

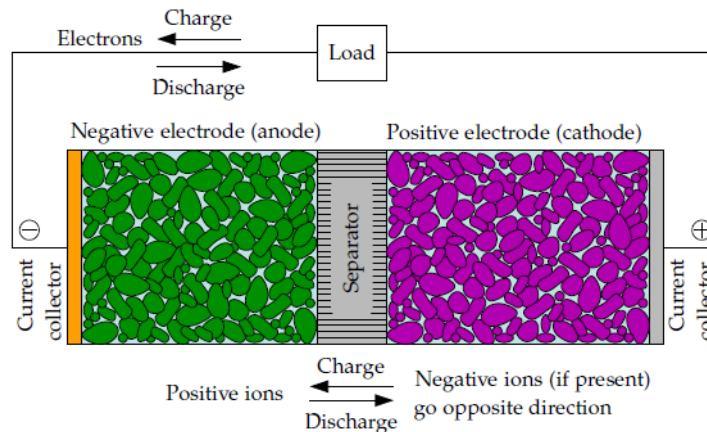


Figure 2.2: Schematic representation of Li-ion cell sandwich [14]

Separator is used to avoid the contact of the electrodes. It is made up of a porous membrane structure soaked in the electrolyte. The separator must have high ionic conductivity and it must be a good electronic insulator [6]. **Current collectors** are used to transport the electrons from one electrode to another electrode. The current collectors must be stable and should not involve in the chemical reactions taking place inside the cell. Copper is used as the current collector for the negative electrode whereas aluminium is used for the positive electrode [29].

2.1.2 Battery packs

A **battery pack** in a vehicle consists of several modules each having many cells in series and parallel. Figure 2.3 shows the expanded view of battery pack having several modules. A battery pack need a battery management system to avoid unsafe operating conditions, protect cells from damage and to prolong the life of the battery [30]. One of the biggest concerns of BEV's is driving range and BMS keeps the battery pack operation optimized to maximize the achievable driving range of the vehicle [31].

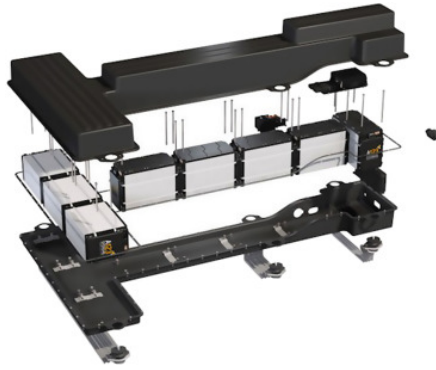


Figure 2.3: Expanded view of battery pack [30]

2.2 Terminologies

- **State of charge (SOC):** It represents the present capacity of the battery compared to the maximum capacity [27].

$$\delta SOC = \frac{1}{Q} * \int_0^t I(t)dt \quad (2.1)$$

where Q is capacity in Ah and I is current in Ampere

- **Open circuit voltage (OCV) :** It is the voltage of the cell when it is not connected to the load. Li-ion cell has OCV between 3-4V depending on the chemistry[12] .
- **Capacity:** The total charge per weight of the cell is referred to as cell capacity. A small cell has less capacity than a larger cell with the same chemistry [6].
- **Energy and power:** The energy of the cells refers to electrical work the cells can perform until the cut-off voltage is reached. Power refers to the rate at which the work has been performed [6].

$$Energy = V(t) * Idt \quad (2.2)$$

$$Power = V(t) * I(t) \quad (2.3)$$

- **C-rate:** It is used to represent the rate of charge or discharge of a cell with respect to its capacity in one hour. For example, for a 20Ah cell, 1 C rate is equal to charge or discharge at 20 A and 5 C rate is equal to charge or discharge at 100 A [27].

3

Methodology

In this chapter, the employed modeling approach, together with different case setups implemented in the thesis are presented.

3.1 Cell electrical-thermal modelling

Figure 3.1 shows a schematic representation of the cell electrical-thermal modelling approach used in the current research work. The current is given as input to the cell. The cell electrical model accounts for the SOC, internal resistance and the terminal voltage. These information are fed to the thermal model which calculates the total heat generated within the cell and hence cell temperature evolution.

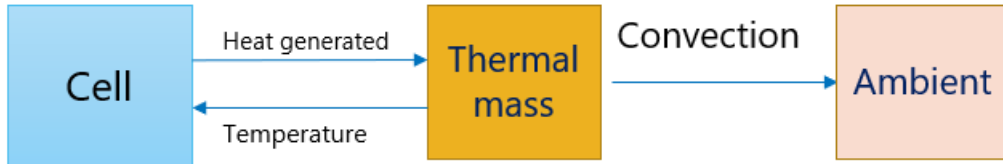


Figure 3.1: Schematic representation of the cell electrical-thermal modelling approach.

3.1.1 Equivalent circuit method (ECM)

The equivalent circuit method uses electric circuit elements to mimic the behaviour of a battery cell. Various circuit elements such as resistors, capacitors and voltage sources are used. It is to be noted that circuit elements don't describe the construction of the cell. In other words, if the cell is opened it is not possible to see resistors, capacitors or voltage sources, etc [8].

There are different ECM models for representing a cell, in this work simple equivalent circuit modelling (the so-called R_{int} model) is considered. Figure 3.2 is a graphical representation of the model. As can be seen, the model includes a voltage source and a resistance. The resistance represents the energy losses. The terminal voltage matches with the open-circuit voltage when it is open but when a load is connected, the voltage is determined as follows [9] :

$$V_t = V_{OC} - R_{int} * I \quad (3.1)$$

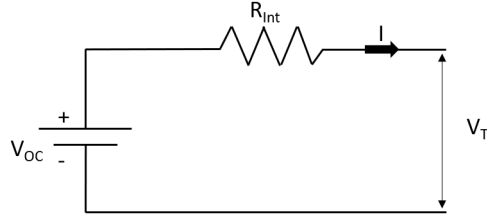


Figure 3.2: Simple equivalent circuit model

3.1.2 Thermal modelling

Even though the cell characteristics depend on the type of materials used, there are some basic physical relationships which have to be considered. Important properties include voltage, capacity, energy and power which are limited by the thermodynamics and kinetics of the chemical reactions. For the redox reactions and temperature dependency of the reactions of the cell, the thermodynamics properties are the basis [6].

Temperature as mentioned earlier is an important parameter that affects the behaviour of the cell and therefore the gradients in the pack. The cell must be operated within an optimum temperature range (20-40°C) to maximize cell performance. At lower temperatures, the conductivity of the ions are low and the internal resistance is high which leads the cell to discharge at a rapid rate and in turn reduces the delivered capacity. At high temperatures the chemical reaction and the side reaction rates increase which negatively influence battery safety and long-term performance (due to the accelerated aging). This highlights the importance of using cooling/heating systems for electric vehicle applications [6].

3.1.2.1 Heat generation

The heat generation inside a cell depends on several factors. The dominant contributors of the generated heat within the cell are the reversible and irreversible heats. The reversible heat is SOC dependent and can either be positive or negative (meaning that the reactions can either be exothermic or endothermic) whereas the irreversible heat is positive. The heat generation is mathematically represented as: [28]

$$\dot{Q} = \dot{Q}_{irr} + \dot{Q}_{rev} \quad (3.2)$$

$$\dot{Q} = I(U - OCV) + IT \frac{dU}{dT} \quad (3.3)$$

To correlate the generated heat to the cell temperature evolution, a lumped energy conservation model is used and is expressed as [32]:

$$\frac{d(\rho c_p T)}{dt} = -hA(T - T_c) + \dot{Q} \quad (3.4)$$

where ρ is the density, c_p is the specific heat, T is cell temperature, T_c is the temperature of cooling medium, h is the heat transfer coefficient, A is the cell outer surface area and \dot{Q} is the total heat generated.

3.2 Lumped pack approach

As mentioned in section 1.4, the current thesis work focuses on analyzing C2C variations in a battery pack, but to have a basic understanding, the modelling is first done on basis of lumped pack approach, where the battery pack is modelled without any discretisation. Figure 3.3 shows the lumped modelling approach.

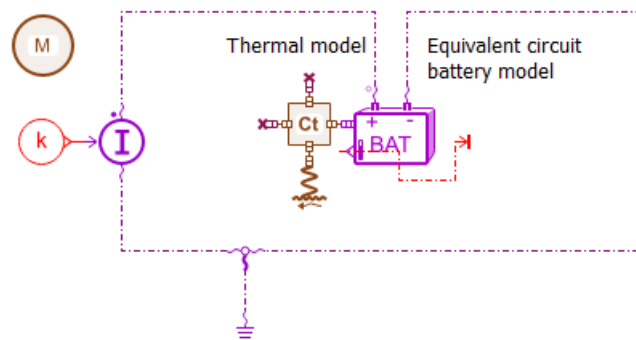


Figure 3.3: Lumped pack model

The battery template is connected to the thermal mass template. The generated heat is sent to the thermal mass from which it is carried by convection through a convection template where different heat transfer coefficients can be given to account for different cooling strategies. If the heat transfer coefficient is between 5-10 W/m²/°C, natural convection is applied [13]. The input current for the model can be given as either a constant value or a current profile (current vs time graph).

3.3 Cell-to-cell discretization approach

By understanding the basic modelling of the battery pack in the above section, the C2C model is implemented. By this approach, the battery is modelled as cells in parallel and series. In the current work, 1S, 5P configuration has been considered. Figure 3.4 graphically represents C2C discretization modelling approach. Each cell is connected with a thermal mass and to a convective heat exchange template. Cells are connected in parallel with interconnection resistance between them [10] [24]. The first cell experiences more current since it is near to the load terminals and is

3. Methodology

subjected to lower R_{IC} . The interconnection resistance is between 1-10 % of cell's internal resistance [10]. In the present work the R_{IC}/R_{int} ratio is 0.06 and therefore the R_{IC} value is 0.06 mOhm. Similar to the lumped pack model, the input current for this model is given either as a constant value or through a current profile. From Kirchhoff's current law, the sum of currents at each junction is zero. The below equations represents the current flow between each cell [24].

$$I_{cell,n} = \begin{cases} I_n - I_{n+1} & n < N \\ I_n & n = N \end{cases} \quad (3.5)$$

From Kirchhoff's voltage law, the sum of voltages around each loop is zero and it is mathematically represented as:

$$V_{t,n} - V_{t,n-1} + 2R_{IC}I_n = 0 \quad (3.6)$$

Terminal voltage of the cell with respect to OCV is defined as:

$$V_t = OCV + R_{cell}I_{cell} \quad (3.7)$$

For 5 cells in parallel, the above equations can be modified to be written in matrix form as:

$$R * \begin{Bmatrix} I_1 \\ I_2 \\ I_3 \\ I_4 \\ I_5 \end{Bmatrix} = A * OCV + B * I_{load} \quad (3.8)$$

The relationship between the loop current and the external load current can be given as:

$$\begin{Bmatrix} I_1 \\ I_2 \\ I_3 \\ I_4 \\ I_5 \end{Bmatrix} = R^{-1}(A * OCV + B * I_{load}) \quad (3.9)$$

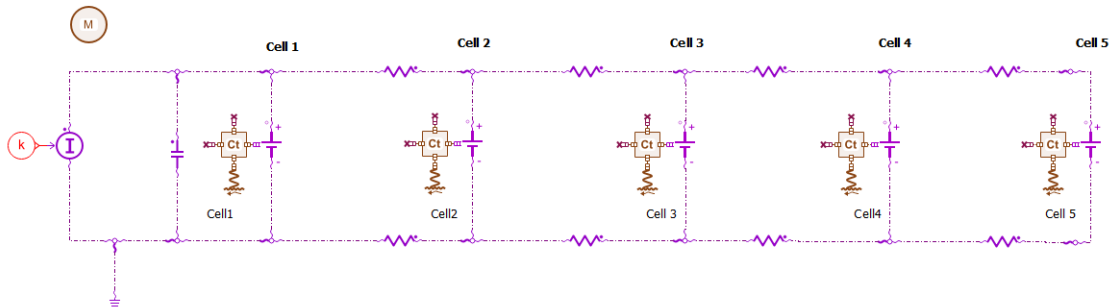


Figure 3.4: Cell-to-cell (C2C) discretization model

3.4 Cell Specification

The cell type under consideration in this work is Lithium nickel manganese cobalt oxide (NMC) prismatic cell. Table 3.1 presents cell specifications required for the purpose of electrical-thermal modeling.

Table 3.1: Cell specification [4]

Parameter	Value
Nominal capacity	42Ah
Nominal voltage	3.7 V
Maximum voltage	4.2 V
Minimum voltage	2.7V
Operating temperature (charging)	0 to 45 °C
Operating temperature (discharging)	-25 to 55 °C
Weight	0.935 kg
Dimensions (WxLxH)	225mm x 225mm x11.8mm

The battery pack comprises one cell in series and five cells in parallel. The total capacity will be 210 Ah. The nominal, minimum and maximum voltage is the same as the cell.

3.5 Case setup

Both the lumped pack model and C2C model are compared for different test cases which are explained as follows.

3.5.1 Case 1- Constant discharge current

To get a basic understanding of how the models behave, the packs are loaded by a constant current. Firstly, both the models are subjected to 1 C discharge current for 2600 seconds and then by 5 C for 350 seconds. Battery cell parameters are kept constant as previously presented in Table 3.1. The initial SOC is considered to be 90% for both models.

3.5.2 Case2- Current profile from test rig

In this case, the models are tested with the current profile from the test rig. The current profile has been obtained from the Siemens Amisem tutorial. The current profile has been used to validate the Li-NMC prismatic cell. The description of the current profile is explained below :

- 0 - 4300 s: continuous charge of 130A
- 4300 - 6200 s: rest phase with no current flowing through the battery
- > 6200 s: typical current from a HEV duty cycle and rest

For this case, the electrical and thermal parameters remains the same and the initial SOC is considered to be 15 % for both the models.

3.5.3 Case 3-WLTP class 3

In this case, a more realistic standardised current profile of the WLTC cycle is used. This current profile has been obtained from the literature [11]. Initial SOC is considered to be 90 % for both the models and the lumped pack model is simulated until the SOC reaches 10 %. For the C2C model, the simulation is stopped when the first cell reaches 10% SOC. Two scenarios are considered for this case :

- Normal conditions: In this case, all parameters remains the same as in case 1 and case 2.
- Faulty conditions: A fault may occur in the module when there is a poor connection of the cell to the busbar or a defective weld [10]. When that fault is next to the terminal its impact is further pronounced. To reflect this condition R_{IC} is assumed to be 15% of cell internal resistance. So in this case R_{IC} is 0.165 mOhm.

4

Results and discussion

In this chapter the results and discussion for different case setups are presented in details.

4.1 Case 1- Constant current source

In this section, the results for the case when constant discharge current of 1 C and 5 C are implemented as input for both lumped pack and C2C models are presented.

4.1.1 1 C discharge

From figure 4.1, it can be seen that, for an individual cell in the lumped pack, the output current is a constant straight line whereas for the C2C model, cell current variations can be seen. The current experienced by the cell in the lumped pack is approximately the average of the cell currents in the C2C model. The first cell experiences higher discharge current initially as it is near to the load terminals. During the end of simulations as the SOC decreases, the current flow changes. Under this condition, the first cell experiences the lowest current as the high value for the cell internal resistance compensates for the low value of the interconnection resistance.

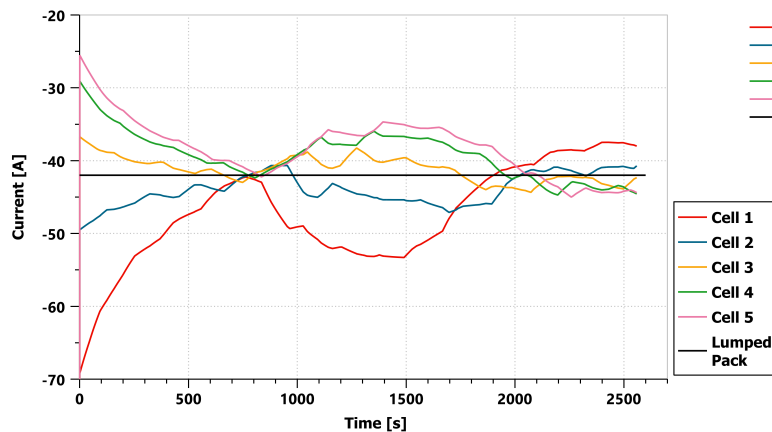


Figure 4.1: Cell discharge current in lumped and C2C packs

Figure 4.2 illustrates that the first cell in the C2C model has 1.5°C higher temperature at the end of discharge compared to the lumped modelling approach meaning

the temperature is underestimated in the lumped pack model. While the lumped pack approach is not capable to capture the temperature gradients within the pack, the C2C approach predicts that the maximum temperature gradient is 3°C between the first and fifth cells.

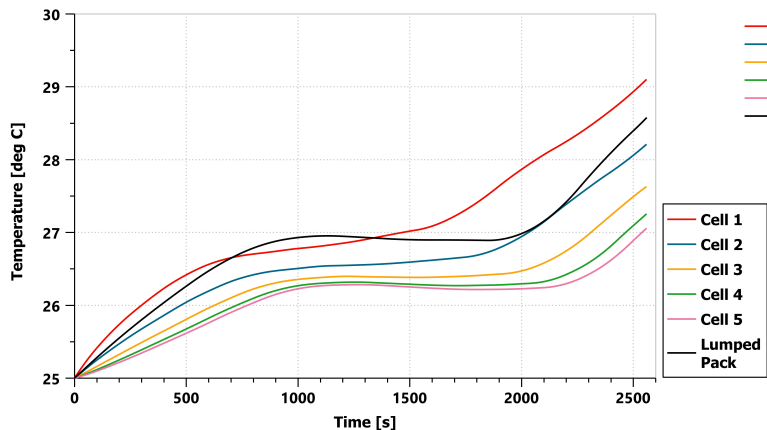


Figure 4.2: Temperature profiles in the lumped and C2C packs

Figure 4.3 shows that, the first cell is discharged faster since it is near the load terminals and experiences higher initial discharging current compared to other cells. At end of discharge, SOC for the lumped pack is 16% whereas the first cell in the C2C model has already reached the SOC of 10%. If the simulation stop criterion is defined based on the lower limit of SOC (e.g. SOC= 10%), then the C2C model stops earlier compared to the lumped pack model.

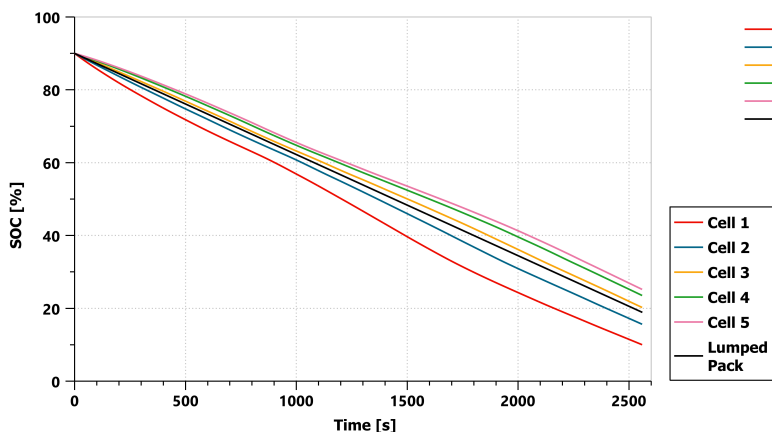


Figure 4.3: SOC profiles for the lumped and C2C packs

4.1.2 5 C discharge

Figure 4.4 shows that the current profile follows the same pattern as for 1 C discharge current scenario, but the variations between the first cell and fifth cell is considerably high which means that the inhomogeneities within the pack are amplified as the input current increases. Also the current experienced by the single cell in the lumped pack is 40% less than the maximum cell current in the C2C model.

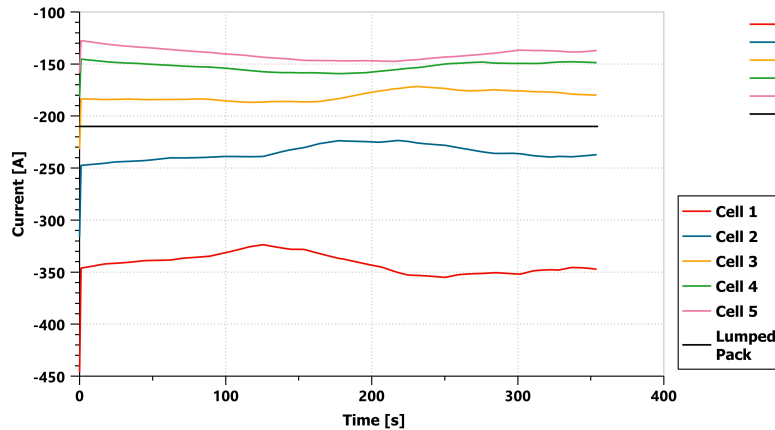


Figure 4.4: Cell discharge current in lumped and C2C packs

Figure 4.5 demonstrates that the maximum temperature gradient is 20°C between the first and fifth cell. The C2C model predicts a temperature gradient of 12°C during the end of discharge.

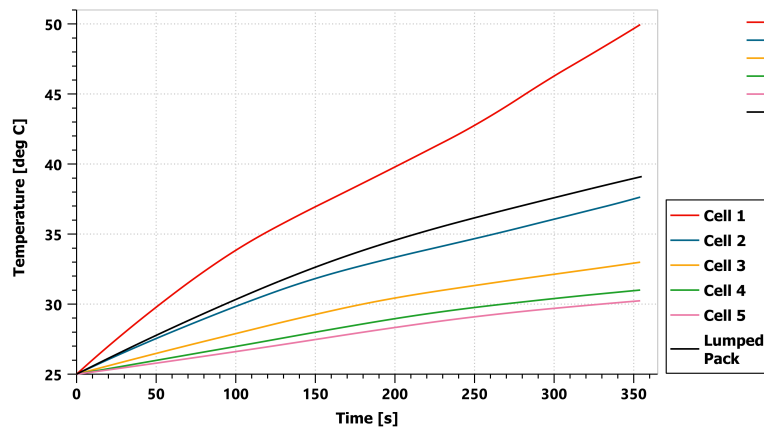


Figure 4.5: Temperature profiles in the lumped and C2C packs

Figure 4.6 shows that the first cell discharges faster than other cells and the variations in cells states of charge are further pronounced compared to the 1 C discharge scenario. At the end of the simulation, the lumped pack has SOC of 40% whereas the first cell in the C2C model has already reached 10%. Therefore, it can be con-

cluded that during high discharge current the lumped pack model overestimates the SOC by 30% compared to the C2C model.

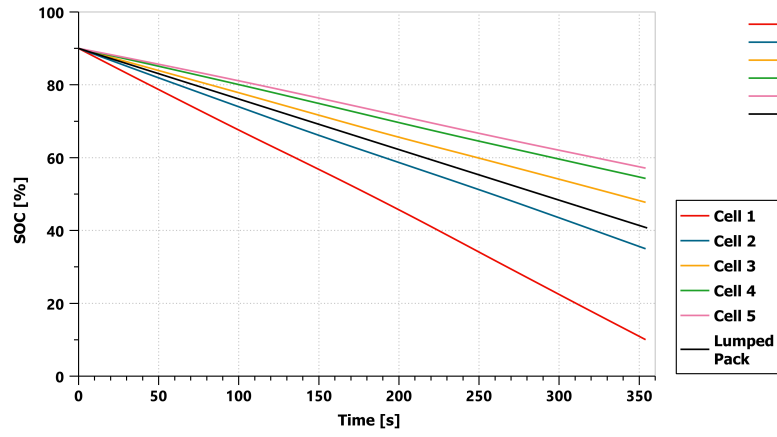
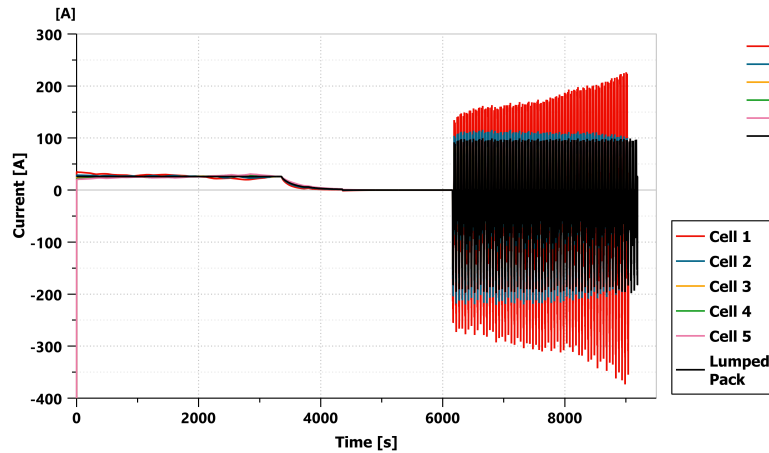


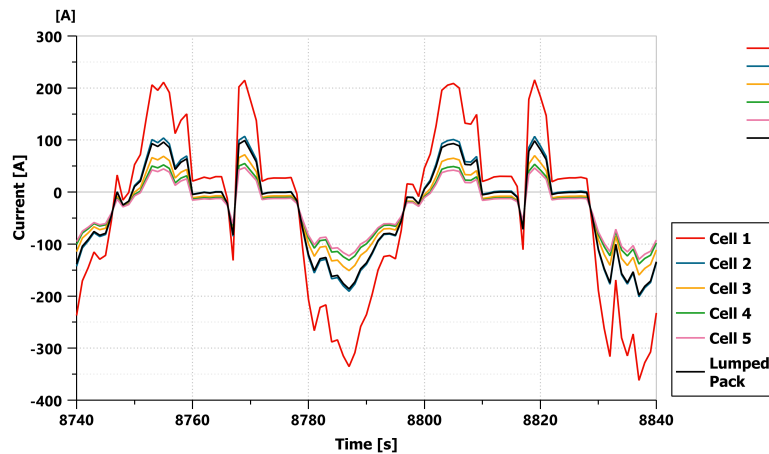
Figure 4.6: SOC profiles for the lumped and C2C packs

4.2 Case 2- Current profile from test rig

Figure 4.7(a) shows the entire current profile for this case. Figure 4.7(b) represents the current profile during the duty cycle. At peak load, the output current of a single cell in the lumped pack is 54% less than the maximum current in the C2C model



(a) Overall current profile for the whole cycle



(b) Current profile at peak load

Figure 4.7: Cell discharge current in lumped and C2C packs

Figure 4.8 represents the temperature profile. The lumped battery pack model underestimates the maximum temperature by 11°C compared to the C2C model. The C2C model predicts a maximum temperature gradient of 20°C within the pack while the lumped model is incapable of providing such an information. Figure 4.9 shows that the C2C pack discharges earlier than the lumped pack by 100 seconds.

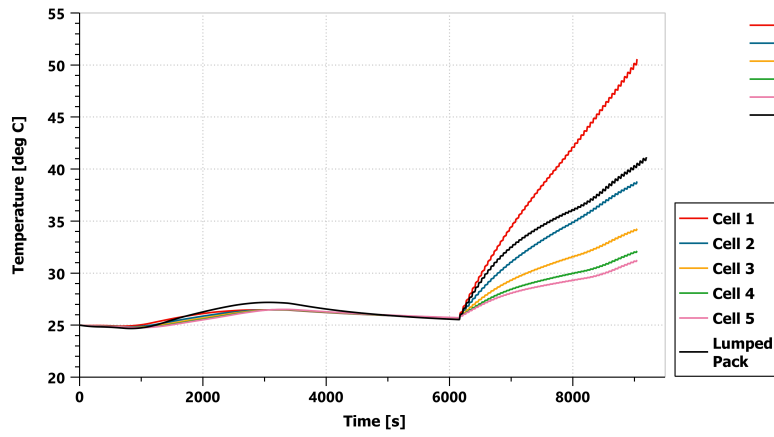


Figure 4.8: Temperature profiles in the lumped and C2C packs

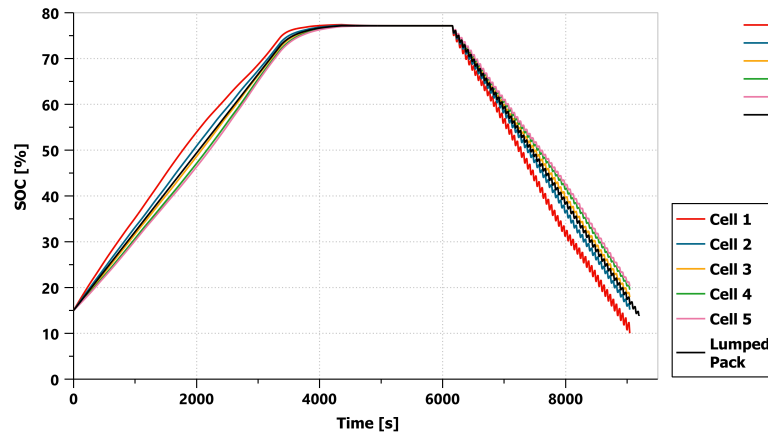


Figure 4.9: SOC profiles for the lumped and C2C packs

4.3 Case 3 - WLTP class 3

This section presents the results for the case when a current profile from the WLTP class 3 cycle is considered as the input for both models. Both the normal condition and the faulty condition scenarios are discussed here.

4.3.1 Normal condition

Figure 4.10 represents the output current for the overall cycle. As expected, the first cell is experiencing higher current levels compared to other cells and the C2C current variation is amplified by the current.

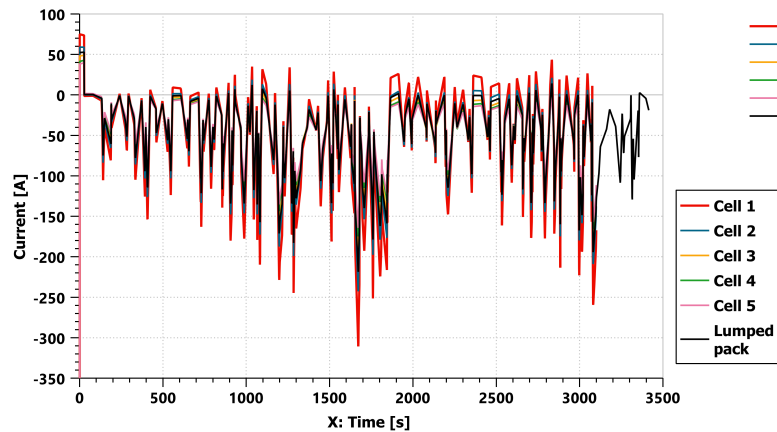


Figure 4.10: Cell discharge current in lumped and C2C packs for overall cycle

Figure 4.11 shows the output current at peak load. It is observed that, when the input current is sufficiently low, the first cell experiences a positive current (i.e. it is charging while others are discharging). This is because as explained earlier, the first branch is next to the load terminals and it discharges at a faster rate and shows lower states of charge than others (SOC profiles refer to the figures confirm this). In the case that the overall battery pack is subjected to very low (almost zero) currents since the first branch has lower states of charge than others, current flows from other branches to the first branch to somehow equalize the battery pack state.

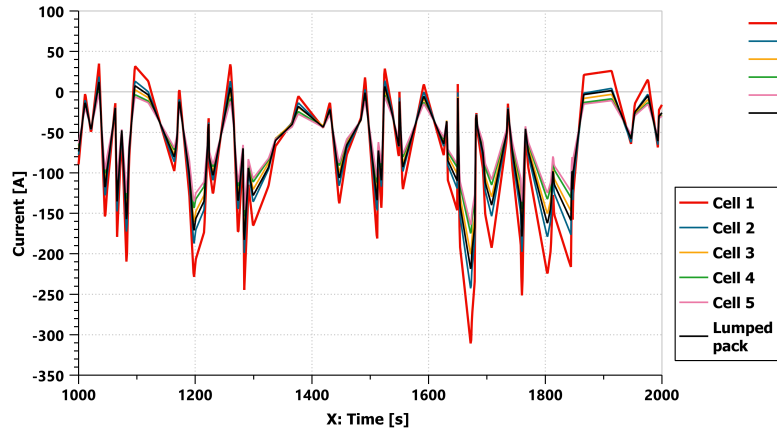


Figure 4.11: Cell discharge current in lumped and C2C packs during peak loads

Figure 4.12 shows the temperature profiles for this case. The lumped battery pack model underestimates the maximum temperature by 4°C compared to the C2C model. The C2C model predicts a maximum temperature gradient of 9°C within the pack.

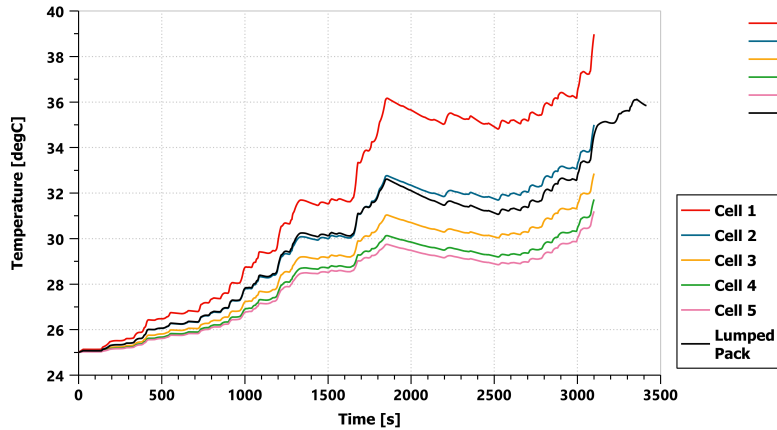


Figure 4.12: Temperature profiles for the lumped and C2C packs

Figure 4.13 illustrates that the C2C model reaches 10% SOC earlier than lumped pack model by 300 seconds. In other words, based on the C2C approach, the battery pack is expected to be discharged 8% earlier compared to the lumped model predictions.

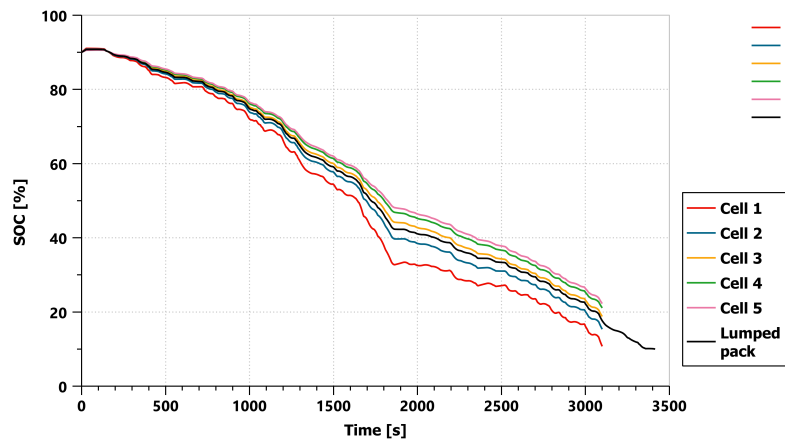
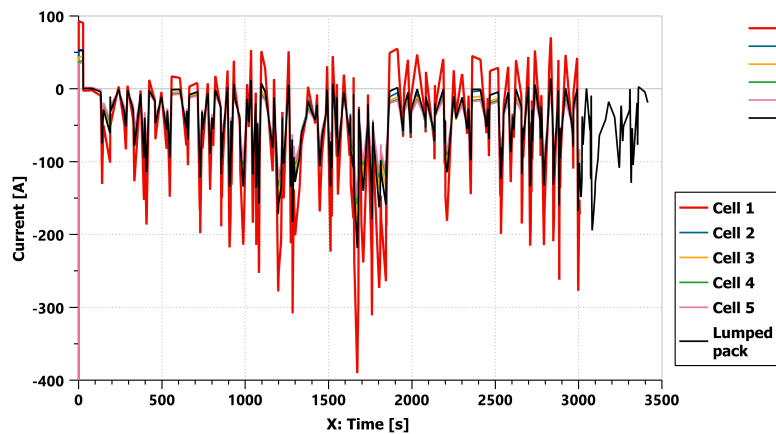


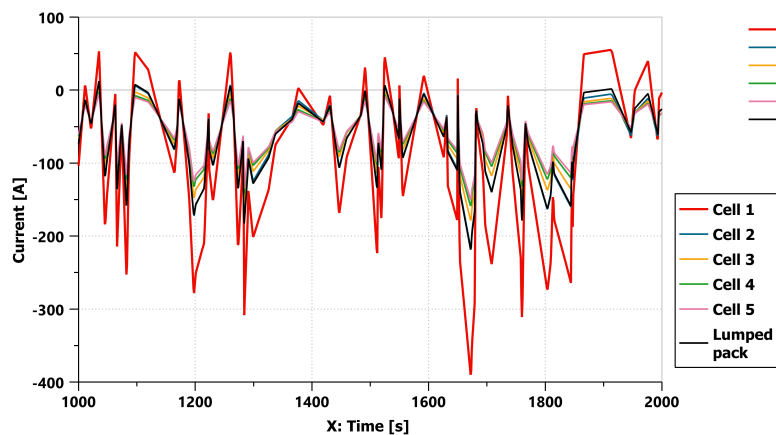
Figure 4.13: SOC profiles for the lumped and C2C packs

4.3.2 Faulty condition

Figure 4.14(a) shows that under faulty condition the discharge current of the first cell is 24% higher during peak load compared to the normal condition and the C2C variations in current profiles are further pronounced.



(a) Current profile for the whole cycle



(b) Current profile at peak load

Figure 4.14: Cell discharge current in lumped and C2C packs

Figure 4.15 shows that, during the peak load current, the temperature increases considerably. The lumped battery pack model underestimates the maximum temperature by 8°C compared to the C2C model. The C2C model predicts a maximum temperature gradient of 13°C within the pack. Figure 4.16 confirms that the first cell discharges quickly and it reaches 10% of SOC around 400 seconds earlier than the lumped pack. When compared to normal condition, the C2C model reaches 10% of SOC around 100 seconds earlier during faulty conditions.

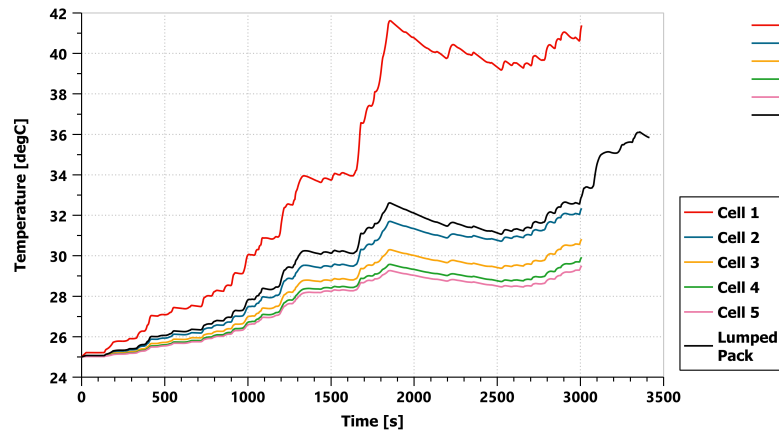


Figure 4.15: Temperature profiles for the lumped and C2C packs

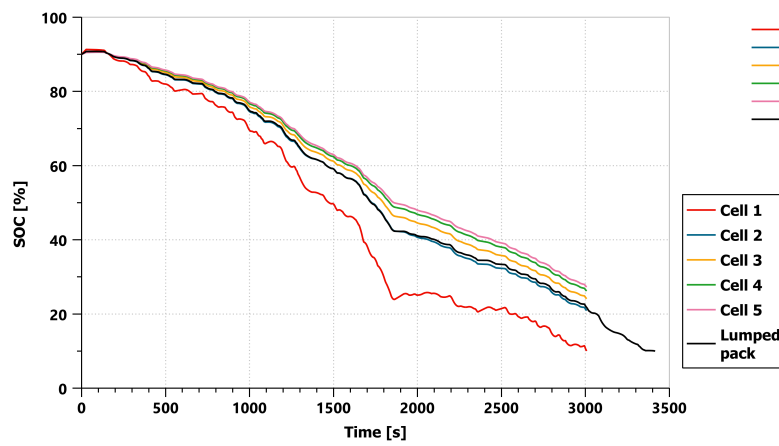


Figure 4.16: SOC profiles for the lumped and C2C packs

5

Conclusion and future work

Modelling large traction battery packs and quantifying inhomogeneities in cell-to-cell operational conditions are of crucial importance for both the pack designers and battery management system developers. Various methods for modelling and performance assessment of battery pack have been developed recently. Lumped pack approach has been useful in many areas (e.g. system level component sizing), but the model predictions are not comprehensive enough since there is no variations between various cells within the pack. In the current research work, a simple lumped pack model was first developed in Siemens Amisem and then a more descriptive model including cell-to-cell variations was developed and compared with the baseline lumped pack model. Both models were tested for the constant current source as well as dynamic current profile obtained from the standardised test method. Results showed that the C2C model provide more comprehensive results compared to the lumped pack model. The maximum temperature in the C2C model was higher compared to the lumped pack model for all of the investigated cases. For the WLTP cycle and under normal condition, the lumped battery pack model underestimate the maximum temperature by $4^{\circ}C$ compared to the C2C model and $12^{\circ}C$ during faulty conditions. When it comes to SOC, the lumped pack model overestimated the discharge time compared to C2C model by 8% during normal conditions and by 11% during faulty conditions. The variations between the cells depend on the value of interconnection resistance and the applied current. It can be concluded that the lumped pack model overestimates the end of discharge SOC for a predefined discharge time and underestimates the maximum temperature within the pack whereas the C2C model is more descriptive and is capable to reflect different real-world working scenarios.

In future work, more detailed modelling of the battery pack can be employed. Currently, a simple equivalent circuit modelling is considered which doesn't consider the dynamic effects. By using 1RC and 2 RC models, the dynamic effects can be visualised. Also the electrochemical modelling approach can be implemented which gives more detailed results by providing access to the cell engineering design and material properties. The battery pack model can be integrated to the vehicle model and real driving simulations can be performed from which vehicle range, energy efficiency and etc. can be extracted. Moreover coupling the developed battery pack model in this work with the pack thermal circuit model, provides detailed insight about battery pack thermal management system design and operation to enhance pack thermal performance.

Bibliography

- [1] Pietrzak, K.; Pietrzak, O. Environmental Effects of Electromobility in a Sustainable Urban Public Transport. *Sustainability* 2020, 12, 1052, doi:10.3390/su12031052.
- [2] Hannah Ritchie and Max Roser, Our world data, *Green house gas emission*. Accessed on: February 17, 2021 <https://ourworldindata.org/greenhouse-gas-emissions>
- [3] Hannah Ritchie Our world data, *Cars, planes, trains: where do CO2 emissions from transport come from?*. Accessed on: February 17, 2021 <https://ourworldindata.org/co2-emissions-from-transport>
- [4] Siemens Amisem. Accessed on: February 25, 2021. <https://www.plm.automation.siemens.com/global/en/products/simcenter/simcenter-amesim.html>
- [5] Master thesis Proposal, Battery pack modelling and performance assessment for electric vehicle application, VEAS division, Chalmers University of Technology
- [6] Berg, Helena; *Batteries for electric vehicles : materials and electrochemistry*, Cambridge University press; DOI- <https://doi.org/10.1017/CBO9781316090978>
- [7] Lino Guzzella and Antonio Sciarretta; *Vehicle Propulsion system*, 3rd edition, Springer; DOI 10.1007/978-3-642-35913-2
- [8] Plett, Gregory ; *Battery management systems, Volume 1* ISBN-13: 978-1-63081-023-8
- [9] Saldana et al., 2019 ; *Analysis of the Current Electric Battery Models for Electric Vehicle Simulation*, *Energies* 2019, 12, 2750; doi:10.3390/en12142750.
- [10] Hosseinzadeh et al., 2020 ; *Quantifying cell-to-cell variations of a parallel battery module for different pack configurations*, WMG, University of Warwick, Coventry CV4 7AL, United Kingdom ; DOI- <https://doi.org/10.1016/j.apenergy.2020.115859>
- [11] Hosseinzadeh et al., 2018 ; *A systematic approach for electrochemical-thermal modelling of a large format lithium-ion battery for electric vehicle application*, WMG, University of Warwick, Coventry CV4 7AL, United Kingdom ; DOI- <https://doi.org/10.1016/j.jpowsour.2018.02.027>
- [12] Balkur Shrishya; *Electro-Thermal modelling of LFP Prismatic cell with SOC estimation model*, Master Thesis, Chalmers University of technology, Chalmers Reproservice.
- [13] E. Prada et al 2012 J. Electrochem. Soc. 159 A1508; *Simplified Electrochemical and Thermal Model of LiFePO₄-Graphite Li-Ion Batteries for Fast Charge Applications*, IFP Energies Nouvelles, Solaize, France ; DOI- 10.1149/2.064209jes

- [14] Stetzel, K., Aldrich, L., Trimboli, M.S., and Plett, G., *Electrochemical state and internal variables estimation using a reduced-order physics-based model of a lithium-ion cell and an extended Kalman filter* Journal of Power Sources, 278, 2015, pp.490–505. DOI:10.1016/j.jpowsour.2014.11.135
- [15] Cheng Zhang et al.,2014;*Battery Modelling Methods for Electric Vehicles - A Review*,DOI: 10.1109/ECC.2014.6862541
- [16] T. Bruen, J. Marco, *Modelling and experimental evaluation of parallel connected lithium ion cells for an electric vehicle battery system*, J. Power Sources 310 (2016) 91e101, DOI-http://dx.doi.org/10.1016/j.jpowsour.2016.01.001.
- [17] L. McCurlie, M. Preindl, A. Emadi, *Fast model predictive control for redistributive lithium ion battery balancing*, IEEE Trans. Ind. Electron. 46 (2017) 1350–1357, DOI-https://doi.org/10.1109/TIE.2016.2611488.
- [18] R. Gogoana, M.B. Pinson, M.Z. Bazant, S.E. Sarma, *Internal resistance matching for parallel-connected lithium-ion cells and impacts on battery pack cycle life*, J. Power Sources 252 (2014) 8–13, DOI-https://doi.org/10.1016/j.jpowsour.2013.11.101.
- [19] R. Xiong, X. Gong, C. C. Mi, and F. Sun, *A robust state-of-charge estimator for multiple types of lithium-ion batteries using adaptive extended Kalman filter*, J. Power Sources, vol. 243, pp. 805–816, Dec. 2012.
- [20] S. Li, C. Mi, and M. Zhang, *A high-efficiency active battery-balancing circuit using multiwinding transformer*, IEEE Trans. Ind. Appl., vol. 49, no. 1, pp. 198–207, Jan./Feb. 2013.
- [21] H. Rahimi-Eichi, U. Ojha, F. Baronti, and M. Chow, *Battery management system: An overview of its application in the smart grid and electric vehicles*, IEEE Ind. Electron. Mag., vol. 7, no. 2, pp. 4–16, Jun. 2013.
- [22] C. Pastor-Fernandez et al.,2016;*A Study of Cell-to-Cell Interactions and Degradation in Parallel Strings: Implications for the Battery Management System*, Journal of Power Sources 329 (2016) 574e585, DOI-http://dx.doi.org/10.1016/j.jpowsour.2016.07.121
- [23] Xianzhi Gong et al.,*Study of the Characteristics of Battery Packs in Electric Vehicles With Parallel-Connected Lithium-Ion Battery Cells*,IEEE TRANSACTIONS ON INDUSTRY APPLICATIONS, VOL. 51, NO. 2, MARCH/APRIL 2015, DOI-10.1109/TIA.2014.2345951
- [24] Hosseinzadeh et al.,2018 ;*Combined electrical and electrochemical-thermal model of parallel connected large format pouch cells*,Journal of Energy Storage 22 (2019) 194–207, DOI-https://doi.org/10.1016/j.est.2019.02.004
- [25] J.B. Goodenough, *Electrochemical energy storage in a sustainable modern society*, Energy Environ. Sci. 7 (1) (2014) 14–18, DOI-https://doi.org/10.1039/C3EE42613K
- [26] Shen, J.; Dusmez, S.; Khaligh, A. *An advanced electro-thermal cycle-lifetime estimation model for LiFePO₄ batteries*. In Proceedings of the 2013 IEEE Transportation Electrification Conference and Expo (ITEC), Detroit, MI, USA, 16–19 June 2013; pp. 1–6.
- [27] Young K., Wang C., Wang L.Y., Strunz K. (2013) *Electric Vehicle Battery Technologies*. In: Garcia-Valle R., Peças Lopes J. (eds) Electric Vehicle Integration

-
- into Modern Power Networks. Power Electronics and Power Systems. Springer, New York, NY. https://doi.org/10.1007/978-1-4614-0134-6_2
- [28] D. Bernardi, E. Pawlikowski, and J. Newman, *A general energy balance for battery systems*, Journal of the electrochemical society, vol. 132, no. 1, p. 5,1985.
- [29] Bidari Saurabh; *Anisotropic Temperature Distribution within Li-ion Cells in EV Batteries*, Master Thesis, Chalmers University of technology, Chalmers Reproservice.
- [30] Warner, John ; *The Handbook of Lithium-Ion Battery Pack Design*, Chemistry, Components, Types and Terminology 2015, Chapter 4, Pages 35-49, <https://doi.org/10.1016/B978-0-12-801456-1.00004-X>.
- [31] Jie Deng et al., *Electric Vehicles Batteries: Requirements and Challenges*, Joule 4, 509–515, March 18, 2020, 2020 Elsevier Inc.
- [32] Astaneh, M., Andric, J., Löfdahl, L. et al (2020) ; *Calibration Optimization Methodology for Lithium-Ion Battery Pack Model for Electric Vehicles in Mining Applications*, Energies 2020, 13(14) <http://dx.doi.org/10.3390/en13143532>
- [33] Korthauer, Reiner ; *Lithium-Ion Batteries: Basics and Applications*, ISBN 978-3-662-53069-6, <https://doi.org/10.1007/978-3-662-53071-9>